doi:10.1111/j.1558-5646.2011.01496.x

PERVASIVE GENETIC INTEGRATION DIRECTS THE EVOLUTION OF HUMAN SKULL SHAPE

Neus Martínez-Abadías,[1,2] Mireia Esparza,[1] Torstein Sjøvold,[3] Rolando González-José,[4] Mauro Santos,[5] Miquel Hernández,[1] and Christian Peter Klingenberg[6]

[1]Secció d'Antropologia, Departament de Biologia Animal, Universitat de Barcelona, Avda. Diagonal 645, 08028 Barcelona, Spain

[2]E-mail: nmartinezabadias@gmail.com

[3]Osteologiska enheten, Stockholms Universitet, SE-106 91 Stockholm, Sweden

[4]Centro Nacional Patagónico, CONICET, Bvd. Brown 2915, U9120ACD Puerto Madryn, Argentina

[5]Departament de Genètica i Microbiologia, Universitat Autònoma de Barcelona, Edifici Cn, 08193 Bellaterra (Barcelona), Spain

[6]Faculty of Life Sciences, University of Manchester, Michael Smith Building, Oxford Road, Manchester M13 9PT, UK

Received October 31, 2010
Accepted October 2, 2011
Data Archived: Dryad doi:10.5061/dryad.12g3c7ht

It has long been unclear whether the different derived cranial traits of modern humans evolved independently in response to separate selection pressures or whether they resulted from the inherent morphological integration throughout the skull. In a novel approach to this issue, we combine evolutionary quantitative genetics and geometric morphometrics to analyze genetic and phenotypic integration in human skull shape. We measured human skulls in the ossuary of Hallstatt (Austria), which offer a unique opportunity because they are associated with genealogical data. Our results indicate pronounced covariation of traits throughout the skull. Separate simulations of selection for localized shape changes corresponding to some of the principal derived characters of modern human skulls produced outcomes that were similar to each other and involved a joint response in all of these traits. The data for both genetic and phenotypic shape variation were not consistent with the hypothesis that the face, cranial base, and cranial vault are completely independent modules but relatively strongly integrated structures. These results indicate pervasive integration in the human skull and suggest a reinterpretation of the selective scenario for human evolution where the origin of any one of the derived characters may have facilitated the evolution of the others.

KEY WORDS: **G matrix, geometric morphometrics, *Homo sapiens*, modularity, quantitative genetics, selection.**

Evolution of morphological structures results from the response to various selection pressures, constraints, gene flow, and random drift, but their relative importance is the subject of continuing debate (Maynard Smith et al. 1985; Arnold 1992; Arthur 2001; Gould 2002; Chenoweth et al. 2010; Futuyma 2010; Klingenberg 2010). Morphological integration coordinates variation among interacting parts of organisms and thus ensures organismal function, but integration is also a widespread source of constraints (Klingenberg 2008; Walsh and Blows 2009). Due to such constraints, selection for localized shape change in a single part of a structure can produce widespread morphological changes because relative constraints deflect the evolutionary response in a direction of morphological space that differs from the direction of selection (Schluter 1996; Klingenberg and Leamy 2001; Klingenberg et al. 2010).

An example of evolutionary change that involved a series of specific morphological alterations is the evolution of the human skull. The transition to bipedal posture was associated with

a forward shift of the foramen magnum, and the subsequent evolution of modern humans included the development of a globular and expanded cranial vault, retraction of the face, and strong cranial base flexion (Aiello and Dean 1990; Lieberman et al. 2004, 2008; Bastir et al. 2010; Lieberman 2011). There is discussion whether changes in cranial features can be considered as adaptive consequences of transitions in locomotion, diet, language, and cognitive abilities (Lieberman 2008, 2011). In support of this viewpoint, recent genetic analyses suggest that many parts of the human genome have experienced positive selection (Hernandez et al. 2011; McLean et al. 2011; Tennessen and Akey 2011), for which the possible phenotypic targets include masticatory musculature (Stedman et al. 2004) and brain development (Evans et al. 2005; Mekel-Bobrov et al. 2005; Pollard et al. 2006; McLean et al. 2011). Nevertheless, there is no compelling evidence of the specific selective forces that shaped the human skull (Lieberman 2008, 2011). An alternative scenario proposes that a few basic developmental changes related to the size and shape of the brain and face may have triggered the whole suite of integrated cranial features of modern humans (Lieberman et al. 2004; Bastir et al. 2010). The debate over whether the evolution of the skull is better understood as a set of localized adaptive changes or as a single change that jointly affected a suite of integrated cranial features relates to the question whether variation in the skull is morphologically integrated or modular (Bastir 2008; Klingenberg 2008; Hallgrímsson et al. 2009; Lieberman 2011).

It is possible to investigate integration and constraints in the human skull by combining the methods of geometric morphometrics (Dryden and Mardia 1998; Klingenberg 2010) and evolutionary quantitative genetics (Lande 1979; Roff 1997; Lynch and Walsh 1998). Genetic integration and constraints can be characterized in the genetic covariance matrix (**G** matrix) of the traits under study (Cheverud 1984; Roff 1997; Kirkpatrick 2009; Walsh and Blows 2009). The **G** matrix for cranial shape can be estimated and genetic integration can be quantified, as it has been done for a range of species (Klingenberg and Leamy 2001; Myers et al. 2006; Martínez-Abadías et al. 2009b; Klingenberg et al. 2010; Adams 2011; Leinonen et al. 2011). This approach requires a sufficiently large sample of skulls with associated genealogical information. The skulls in the ossuary of Hallstatt (Austria) provide a unique opportunity to conduct this kind of study because skulls are individually identified and church records can be used to reconstruct genealogical relationships (Sjøvold 1984; Martínez-Abadías et al. 2009a). This information makes it possible to estimate directly the **G** matrix for skull shape and provides a crucial advantage over previous studies of human evolution that have used phenotypic covariance structure as a proxy for genetic data (Ackermann and Cheverud 2004; Roseman 2004; Weaver et al. 2007; Perez and Monteiro 2009; von Cramon-Taubadel 2009; Betti et al. 2010). Quantitative genetic studies on cranial traits in humans have been conducted before (Johannsdottir et al. 2005; Carson 2006; Sherwood et al. 2008; Martínez-Abadías et al. 2009a), but this is the first analysis of genetic integration of shape in the human skull.

Here we analyze quantitative genetic variation of skull shape in the Hallstatt population. Our analyses provide evidence for strong integration throughout the skull. Simulations of localized selection for the principal derived characters in the human skull consistently produce global responses throughout the skull and thus reveal that genetic integration has a major effect on the resulting shape change. We also test the hypothesis that the face, neurocranium, and cranial base are completely independent morphological modules, but the statistical test used rejects the hypothesis. This strong genetic and developmental integration in the skull suggests an evolutionary scenario in which the origin of any one of the derived traits in the human skull may have facilitated the evolution of others.

Methods

DATA COLLECTION AND MORPHOMETRIC ANALYSIS

The sample used in this study is from the ossuary of Hallstatt (Austria) and includes skulls of individuals buried in the Catholic churchyard of the town. As a local tradition, skeletal remains were recovered, various decorations were painted on the skulls, and skulls were subsequently stored in the ossuary. Most decorations include the names of the individuals, so that parish records make it possible to reconstruct genealogical relationships. More detailed information about the sample and the methods used for obtaining genealogical information can be found elsewhere (Sjøvold 1984; Martínez-Abadías et al. 2009a).

The sample includes 390 complete skulls that are mainly adult individuals (91% adults, 9% subadults) from both sexes (41% females; 59% males) born between 1707 and 1885. A small proportion of skulls was classified as either visibly asymmetric (8.2%) or as having slight dysmorphologies possibly related to craniosynostosis (3.8%). Strongly dysmorphic skulls were excluded from consideration (for further details, see Martínez-Abadías et al. 2009a).

We characterized skull shape with 29 anatomical landmarks distributed over the left side of the skull (Fig. 1; and Table S1). The landmark coordinates were recorded with a Microscribe 3D digitizer.

Geometric morphometric techniques were used to capture size and shape variation from the coordinate data. To extract shape information, we used a generalized full Procrustes superimposition (Dryden and Mardia 1998). Skull size was recorded as centroid size, the square root of the sum of squared distances of all the landmarks of a skull from their center of gravity (Dryden and Mardia 1998). A principal component (PC) analysis was used

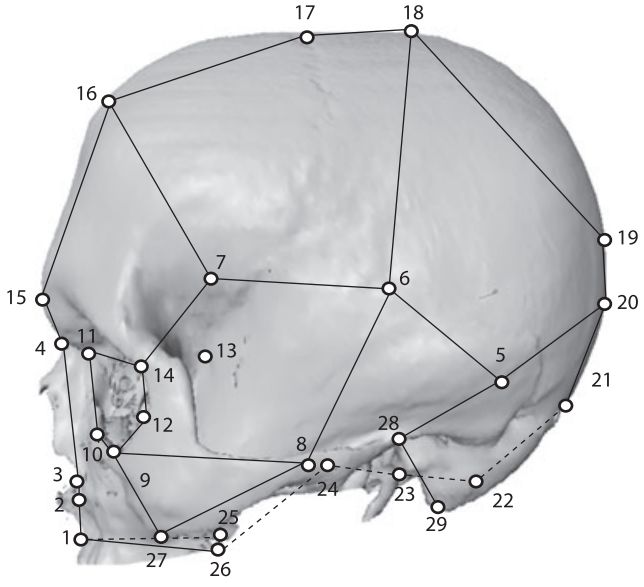

Figure 1. Landmarks and wireframe superimposed on a lateral view of a human skull. The landmarks connected by dashed lines (in the midline of the skull) as well as landmark 13 (inside the orbit) are not visible from this view. The image of the skull is derived from a CT scan and has been morphed to correspond to the mean shape of the skulls in the sample used in this study.

to reduce the dimensionality of the data that was necessary due to computational limitations in the quantitative genetic analysis. The first 32 PCs accounted for 89.6% of shape variation and were used for the quantitative genetic analyses. All morphometric analyses were done with MorphoJ (Klingenberg 2011).

To assess measurement error, a subset of 91 skulls was measured a second time and both replicate measurements were analyzed in a preliminary Procrustes analysis of variance (ANOVA) (Klingenberg and McIntyre 1998). The Procrustes sum of squares for variation among individuals exceeded that of measurement error by a factor of 11.6, and thus indicates that measurement error is small overall.

QUANTITATIVE GENETIC ANALYSIS

Genealogies were compiled from complete church records from 1602 to 1900 and included 350 individuals with preserved skulls and 1089 additional individuals related to them. Restricted maximum likelihood methods (REML) based on an individual-based model (also known as the "animal model"; Lynch and Walsh 1998; Kruuk 2004; Kruuk et al. 2008; Wilson et al. 2010) were used to estimate the additive genetic and phenotypic covariance matrices with the software package Wombat (Meyer 2007). The shape information was entered into the computations as the scores for the first 32 PCs from the initial PCA (this number reflects the limitations of the software). The statistical model included centroid size as a covariate (thereby removing allometric effects from the shape variation), and sex and deformation status (no deformation, asymmetric or dysmorphic) as fixed effects. Analyses using the same model that were run with the VCE6 software (Groeneveld et al. 2008) produced results that were closely similar.

To examine the main patterns of genetic variation, which are the shape features corresponding to directions of "least resistance" (Schluter 1996), we conducted a PC analysis of the additive genetic covariance matrix (**G** matrix) for cranial shape. For comparison, we also conducted a separate PCA for the phenotypic covariance matrix (**P** matrix). To quantify the overall relatedness of the **G** and **P** matrices, we computed the matrix correlation between them and evaluated it with a matrix permutation test, as adapted for geometric morphometrics (Klingenberg and McIntyre 1998).

HYPOTHETICAL SELECTION

To explore the evolutionary consequences of genetic integration in the skull, we predicted responses to hypothetical selection regimes (Klingenberg and Leamy 2001; Martínez-Abadías et al. 2009b; Klingenberg et al. 2010). This approach uses the multivariate version of the breeders' equation, $\Delta\boldsymbol{\mu} = \mathbf{G}\boldsymbol{\beta} = \mathbf{G}\mathbf{P}^{-1}\mathbf{s}$, where $\Delta\boldsymbol{\mu}$ is the evolutionary change in the mean shape in response to selection, **G** is the additive genetic covariance matrix, **P** is the phenotypic covariance matrix, $\boldsymbol{\beta}$ is the selection gradient, and **s** is the selection differential (Lande 1979).

To test whether selection for specific features of the skull elicits a localized response of just the selected region or an integrated response of the entire skull, we designed five hypothetical selection gradients that represent the principal derived features of the modern human skull separately as localized shape changes (Aiello and Dean 1990; Lieberman et al. 2004, 2008; Lieberman 2011). This approach simulates what would happen if a particular selection regime was applied to the Hallstatt population. Although this is not a direct evaluation of past events in the human evolutionary lineage, it makes it possible to assess the selection response under the assumption of a conserved genetic and developmental basis for cranial shape. Given that no genetic data are available for the relevant ancestral populations, data from recent humans such as the Hallstatt population provide the best available evidence. Note that these are purely "what-if" scenarios and do not imply claims that the shape features used for the hypothetical selection gradients are indeed providing fitness advantages (quite to the contrary, the adaptive contexts of all these evolutionary changes are poorly understood; e.g., Lieberman 2008).

The selection gradients were simulated as localized shape changes. To enhance our ability to determine whether localized selection leads to integrated changes in the entire skull and to distinguish the effects of different selection regimes, we defined these shape changes as relative shifts in the positions of only a minimal number of landmarks. We first describe these shape changes

and then specify how the selection gradients were computed from them.

Shift of the foramen magnum

The transition to bipedal locomotion was associated with a relative shift of the foramen magnum in a more anterior position, located under the braincase, and oriented downward. By contrast, in most nonhuman primates, the foramen magnum is located far back on the skull and has a more posterior-facing orientation. The relative position of the foramen magnum in humans facilitates balancing of the head in an upright posture and while running (Jaanusson 1987; Lieberman 2008, 2011). To simulate the relative forward shift of the foramen magnum, the two midline points of the foramen magnum (opisthion, no. 22, and basion, no. 23) were moved forward (see Table S3).

Cranial base flexion

Another feature of the modern human skull is the flexion of the cranial base that results in a more ventrally oriented face and a shortened pharyngeal space behind the palate (Lieberman et al. 2000b, 2008; Bastir et al. 2010; Lieberman 2011). Traditionally, analyses of cranial flexion have focused on endocranial aspects, and cranial base flexion has usually been quantified by the angle nasion-sella-basion, although other angles have been used and can capture different anatomical aspects of cranial base flexion (Lieberman et al. 2000b; Bastir et al. 2010). Because our study only included external landmarks, we had to focus on effects of cranial base flexion on external parts of the skull and therefore considered hormion (no. 24) that is the landmark closest to the axis of flexion. Increased flexion will raise structures near this axis relative to surrounding structures, so we simulated it as a localized shape change by a relative upward shift of hormion (Table S4).

Facial retraction

Humans have an unusually flat face that is located under the anterior part of the braincase. This arrangement contrasts with the more anteriorly oriented face of other primates, which have a much more pronounced snout. To simulate facial retraction, the landmarks of the nasomaxillary complex were moved backwards into a more posterior position jointly as a facial block (Table S5).

Expansion of the cranial vault

One of the most pronounced features of modern human skulls is the expanded and rounded cranial vault that is associated with the drastic increase in brain volume. This is a shape change that affects large parts of the skull jointly and it is therefore not optimal for assessing whether localized selection produces integrated responses. Therefore, to simulate selection for a larger and more globular cranial vault as a more localized shape feature, we designed two different selection gradients, one for the anterior neurocranial region, and another one for the posterior region. Enlargement and globularity of the anterior neurocranial region were represented by an anterior and upward shift of metopion (no. 16), a lateral shift of pterion (no. 7), and smaller shifts of glabella (no. 15) and bregma (no. 17; see Table S6). Enlargement of the posterior neurocranial region was depicted in a similar way by moving vertex (no. 18), lambda (no. 19), opisthocranion (no. 20), inion (no. 21), euryon (no. 6), and asterion (no. 5) away from the center of the skull (see Table S7).

Computing and applying the selection gradients

Shifts of landmarks used for defining hypothetical selection gradients, as described above, can produce changes in the size, position, and orientation of the resulting configuration, that is, changes of aspects other than shape. Because only shape variation is included in the quantitative genetic analysis, such extra variation may produce the false appearance of constraints. To ensure that selection gradients were proportional to shape differences, we projected the specified landmark shifts onto the tangent space to shape space (Klingenberg et al. 2010). This can result in smaller shifts of other landmarks to compensate for changes in overall position, orientation, and size, but all those shifts are much smaller than the shifts of the "focal" landmarks (recall, the shape change is characterized by the relative shifts of landmarks against one another).

Selection gradients for selection on shape are not shape changes (Klingenberg and Monteiro 2005). Selection gradients express the change in relative fitness per unit of change in shape (Lande 1979; Lande and Arnold 1983). Accordingly, they are not in units of Procrustes distance and, because shape variation within populations tends to be small, selection gradients for normal selection intensities tend to exceed the lengths that are possible for shape vectors. For instance, for the mean standardized selection gradient of 0.22 estimated by Kingsolver et al. (2001) and the standard deviation of 0.022 units of Procrustes distance for the PC1 scores of our data, the selection gradient would have a length of 10 and would go far beyond the projection of shape space onto the tangent space. Accordingly, we used a scalar conversion factor to ensure that the selection gradient was proportional to the specified shape change, so that $\boldsymbol{\beta} = c\mathbf{b}$, where $\boldsymbol{\beta}$ is the selection gradient, $\mathbf{b}$ is the shape vector indicating the direction of selection and c is a proportionality constant (Klingenberg et al. 2010). The use of this conversion makes it possible to analyze direct selection, because the selection gradient accounts for the effects of those shape features that are not the target of selection, but are phenotypically correlated (Lande and Arnold 1983).

The magnitude of selection gradients was scaled so that the standardized selection gradients for the corresponding shape variables were 1.0, that is, one unit of change in relative fitness per standard deviation of the shape variable corresponding to the

vector **b** (Klingenberg et al. 2010). If **b** is chosen to have unit length (i.e., $\mathbf{b}^{\mathrm{T}}\mathbf{b} = 1.0$, where the subscript "T" stands for the transpose), the standard deviation of the corresponding shape variable is $\sigma = (\mathbf{b}^{\mathrm{T}}\mathbf{P}\mathbf{b})^{0.5}$ and the constant c can be set to $1/\sigma$, so that the standardized selection gradient for the shape variable is 1.0 (note that the length of the corresponding selection gradient $\boldsymbol{\beta}$ usually will not be 1.0; for shape variables measured in units of Procrustes distance, where σ is normally much less than 1.0, the vector $\boldsymbol{\beta}$ can be much longer). A standardized selection gradient of 1.0 corresponds to a high intensity of selection, but is well within the range of empirical data on selection in natural populations of a wide range of organisms (Hoekstra et al. 2001; Kingsolver et al. 2001). Because the multivariate breeders' equation is linear, the magnitude of the selection gradient has no effect on the direction of the predicted response and therefore does not affect our conclusions concerning genetic integration of shape. The numerical values of the selection gradients are provided in the Supplementary Information (Tables S3–S7, in relation to the orientation of the mean configuration as in Table S2), and graphical displays of the corresponding shape changes are provided with the results of the respective analyses.

After applying the multivariate breeders' equation, we decomposed the total predicted response to selection into two components: the direct response in the direction of the selection gradient and the correlated response perpendicular to it (Klingenberg and Leamy 2001; Martínez-Abadías et al. 2009b; Klingenberg et al. 2010). The relative magnitudes of the direct and correlated responses or, equivalently, the angle between the directions of the total response and the selection gradient (and thus also of the direct response) indicates the effect of relative genetic constraints on the selection response (Klingenberg and Leamy 2001; Klingenberg et al. 2010). The total response and its components are all shape changes and can therefore be measured in units of Procrustes distance. In our diagrams of selection responses, we exaggerated the corresponding shape changes by a factor of 10 for better visibility.

ANALYSIS OF MODULARITY

To examine the modularity of the skull, we examined the hypothesis that the face, the cranial base, and the cranial vault are distinct modules. If this hypothesis is true, each of these regions should be highly integrated internally and relatively independent of the other two regions. Modularity can be assessed by analyzing covariation among subsets of landmarks (Klingenberg 2008, 2009). If the subdivision of the cranial landmarks into subsets corresponds to or closely resembles the true modules, covariation among subsets should be weak because the strong integration within modules does not contribute to covariation between subsets. In contrast, if the subsets do not correspond to the true modules, the strong within-module integration contributes to the covariation among

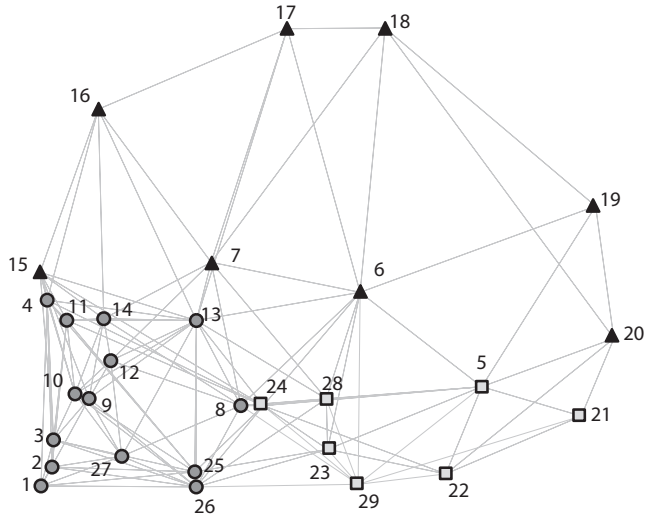

Figure 2. Hypothesis of modularity. The different symbols identify the hypothetical module to which each landmark belongs: face (circles), cranial base (squares), or cranial vault (triangles). The gray lines connecting landmarks represent the adjacency graph used to define spatially contiguous partitions of the landmarks (Klingenberg 2009). A subset of landmarks is considered to be spatially contiguous if all its landmarks are connected by these lines (without passing through any landmarks belonging to a different subset).

subsets that will therefore be stronger. Overall, it is expected that covariation among subsets is weaker for subsets corresponding to the true modules than for other partitions of the landmarks into subsets (Klingenberg 2009). This approach has been used in a growing number of studies to test hypotheses of modularity (e.g., Hallgrímsson et al. 2009; Bruner et al. 2010; Drake and Klingenberg 2010; Ivanović and Kalezić 2010; Klingenberg et al. 2010; Jamniczky and Hallgrímsson 2011; Jojić et al. 2011).

To assess the hypothesis of modularity, we computed the multiset *RV* coefficient (Klingenberg 2009) to quantify the strength of association between subsets of the landmarks corresponding to the face, the cranial base, and the cranial vault (Fig. 2). The multiset *RV* coefficient is a generalization of the *RV* coefficient (Escoufier 1973) that is a measure of association between two sets of variables and can be interpreted as a multivariate analogue of the squared correlation coefficient (R^2, as it is widely used, e.g., in regression analysis). The multiset *RV* coefficient is obtained by averaging the pairwise *RV* coefficients for all possible pairings of sets (Klingenberg 2009). The multiset *RV* coefficient was computed from the Procrustes-aligned coordinates of the landmarks of the face, the cranial base, and cranial vault (Fig. 2; containing 14, 7, and 8 landmarks, respectively), and for 10,000 random partitions of the total set into random subsets containing the corresponding numbers of landmarks.

It might be objected that the total set of random partitions is not a fair basis for comparison, because it contains partitions with

one or more subsets that are spatially disjointed. For instance, a subset of landmarks may contain the anteriormost and posteriormost landmarks as separate clusters, but not the landmarks located between them. Such a disjoint subset of landmarks may not be considered as a realistic candidate for being a module because it lacks the spatial cohesion that provides its individuality as a module and because integration through tissue-bound mechanisms such as cell–cell signaling cannot occur between spatially separated units. For this reason, in addition to the comparison with unrestricted random partitions, we also conducted comparisons that were limited to subsets of landmarks that were spatially contiguous (Klingenberg 2009). A subset of landmarks was considered spatially contiguous if all its landmarks were connected by the edges of the adjacency graph (Fig. 2; Klingenberg 2009). For this analysis, multiset *RV* coefficients were computed for 10,000 partitions in which all three subsets were spatially contiguous according to this definition.

Results

PATTERNS OF GENETIC VARIATION

PC analysis showed that the phenotypic variation in the sample is distributed across many dimensions of the shape space: the first PC accounts for 12.8% of the total variance in the **P** matrix and the subsequent eigenvalues decline gradually (Fig. 3A). For the genetic covariance matrix, variation is more concentrated and the decline is steeper (Fig. 3B).

The shape changes associated with the first PC of the **G** matrix (Fig. 3C) include a retraction of the lower face, an expansion of the anterior cranial vault, a forward and upward rotation of the foramen magnum, as well as a flexion of the skull about the region of the hormion (no. 24; this description is of a change of the PC1 in the positive direction). The second PC (Fig. 3D) combines a retraction of the orbital region and upper face, a greater development of the frontal and occipital portions of the cranial vault resulting in an expansion of the braincase, and a forward shift of the foramen magnum. These changes can all be related to the primary derived traits of modern human skulls: the forward shift of the foramen magnum, retraction of the face, flexion of the cranial base, and expansion of the cranial vault.

The matrix correlation between the **P** and **G** matrices is fairly high: the matrix correlation including diagonal blocks of within-landmark variances and covariances is 0.85 ($P < 0.0001$), whereas it is 0.75 ($P < 0.0001$) without the diagonal blocks and thus including only the covariances among landmarks. This indicates that, overall, the **P** and **G** matrices resemble each other quite closely.

HYPOTHETICAL SELECTION

The first simulation concerns the forward shift of the foramen magnum (Fig. 4). The total response to selection affects the entire

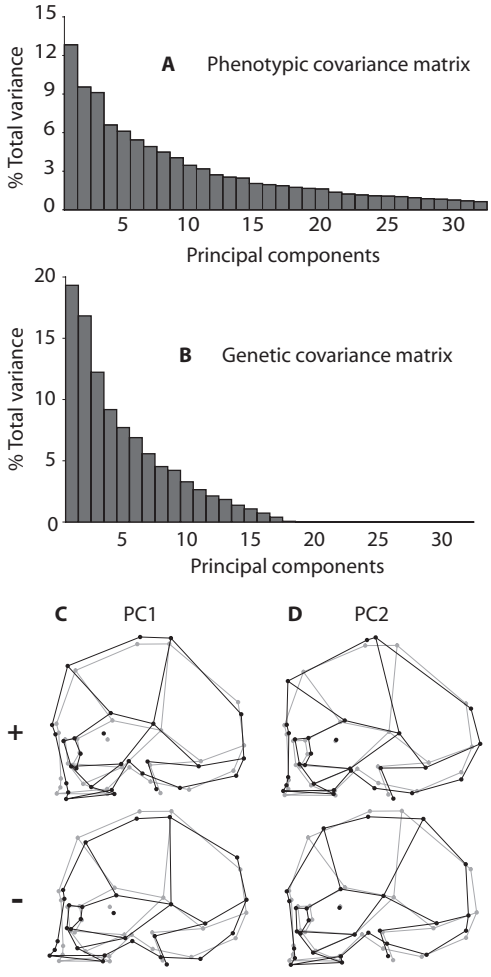

Figure 3. Principal component analysis of the phenotypic and genetic covariance matrices. (A, B) Eigenvalues of the P and G matrices as percentages of the total variance in the respective covariance matrix. (C, D) Shape changes associated with the first and the second PCs of the G matrix (the gray wireframes show the overall mean shape configuration). Top: change in the direction with positive sign; bottom: change in the direction with negative sign.

skull and encompasses the complete set of derived features of modern humans: cranial base flexion, facial retraction, and expansion of the entire cranial vault. This total response consists of a direct response that is localized to the landmarks of the foramen magnum and a correlated response affecting most of the landmarks throughout the skull. The magnitude of the correlated response exceeds that of the direct response, which means that the direction of response has been deflected from the direction of the selection gradient by an angle of over 56° (Fig. 4). This indicates that genetic constraints have a substantial effect on the response to selection.

For cranial base flexion (Fig. 5), the correlated response far exceeds the direct response, showing a very strong effect of

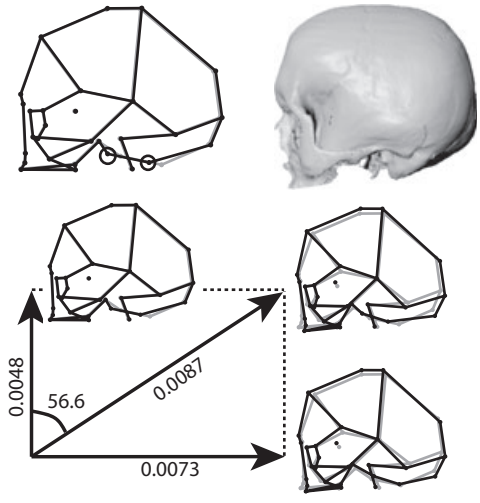

Figure 4. Hypothetical selection on skull shape: shift of the foramen magnum. Top left: the selection gradient, which was defined as a relative forward shift of the two landmarks of the foramen magnum (change from the gray to the black wireframe, with focal landmarks circled). Top right: the total response to selection, amplified by a factor of 10 and visualized as a morphed surface of a skull (deformed from the mean shape shown in Fig. 1). Lower half: decomposition of the total response (diagonal arrow and upper-right wireframe diagram) into the direct response in the direction of the selection gradient (vertical arrow and associated wireframe diagram) and the correlated response (horizontal arrow and lower-right wireframe diagram). In each of the wireframe graphs, the change from the gray to the black wireframe shows the respective response component, amplified by a factor of 10 for better visibility. The amount of shape change for the components of the response are indicated in units of Procrustes distance.

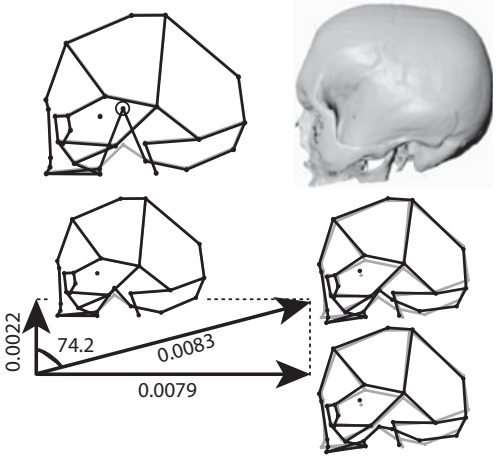

Figure 5. Hypothetical selection on skull shape: cranial base flexion. Top left: the selection gradient, which was defined as a relative upward shift of hormion (change from the gray to the black wireframe and circled landmark). Top right: the total response to selection, amplified by a factor of 10 and visualized as a morphed surface of a skull. Lower half: decomposition of the total response into its components of direct and correlated response. For further details, see legend to Figure 4.

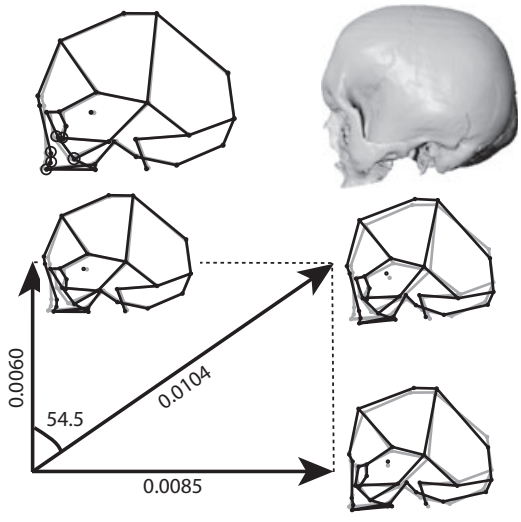

Figure 6. Hypothetical selection on skull shape: facial retraction. Top left: the selection gradient, which was defined as a relative backward shift of a block of facial landmarks (change from the gray to the black wireframe and circled landmark). Top right: the total response to selection, amplified by a factor of 10 and visualized as a morphed surface of a skull. Lower half: decomposition of the total response into its components of direct and correlated response. For further details, see legend to Figure 4.

constraints. In addition to cranial base flexion, the total response consists of a forward and upward shift of the foramen magnum, retraction of the face, and a general expansion of the braincase (including a widening of the posterior region, not visible in Fig. 5).

In the simulation of selection for facial retraction (Fig. 6), again, the correlated response is greater than the direct response. Along with the facial retraction we selected for, the total response also includes the shift of the foramen magnum, cranial base flexion, and an anterior expansion of the braincase.

The simulation of selection for a larger and more globular anterior cranial vault (Fig. 7) produces a total response that again exceeds the direct response and includes the whole suite of changes. When simulating enlargement of the posterior neurocranial region (Fig. 8), the direct response is greater than the correlated response and the deflection from the selection gradient to the total response is less than 45°. The total response is primarily an expansion of the entire cranial vault; the other changes are difficult to interpret because a slight forward movement of the foramen magnum and reduction of the face were already included in the selection gradient as a consequence of the projection to tangent space.

MODULARITY IN THE SKULL

To test the hypothesis of modularity for the face, cranial base, and cranial vault, we compared the multiset *RV* coefficient for this partition of landmarks (Fig. 2) with alternative partitions

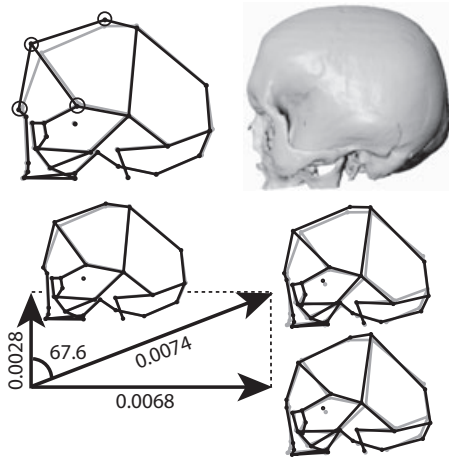

Figure 7. Hypothetical selection on skull shape: anterior enlargement of the cranial vault. Top left: the selection gradient, which was defined as relative forward, upward, and lateral shifts of the landmarks of the anterior cranial vault (change from the gray to the black wireframe and circled landmarks). Top right: the total response to selection, amplified by a factor of 10 and visualized as a morphed surface of a skull. Lower half: decomposition of the total response into its components of direct and correlated response. For further details, see legend to Figure 4.

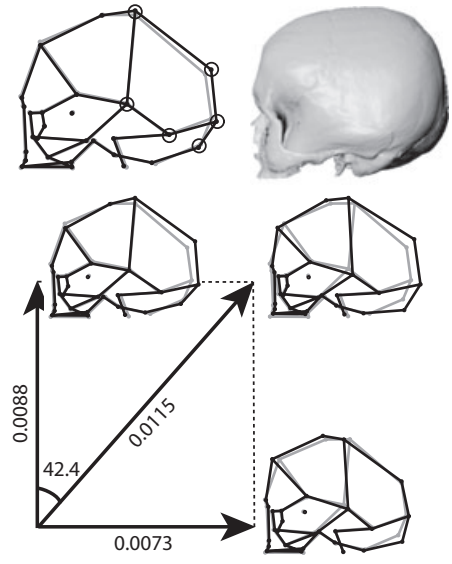

Figure 8. Hypothetical selection on skull shape: posterior enlargement of the cranial vault. Top left: the selection gradient, which was defined as relative upward, lateral, and posterior shifts of the landmarks of the posterior cranial vault (change from the gray to the black wireframe and circled landmarks). Top right: the total response to selection, amplified by a factor of 10 and visualized as a morphed surface of a skull. Lower half: decomposition of the total response into its components of direct and correlated response. For further details, see legend to Figure 4.

(Klingenberg 2009). For the **G** matrix, the multiset *RV* coefficient is 0.52 that is near the mode of the distribution of multiset *RV* coefficients among random partitions of landmarks (Fig. 9A, left diagram): 6072 of 10,000 random partitions yield weaker associations among subsets. If the comparisons are restricted to partitions into spatially contiguous subsets only, 4070 of 10,000 random partitions show weaker associations (Fig. 9A, right diagram). Because the association among the three subsets is near the center of the distribution of multiset *RV* coefficients, not near the lower extreme, the hypothesis of modularity is rejected for the **G** matrix.

For the **P** matrix, the multiset *RV* coefficient for the three subsets of landmarks is 0.27, and 7101 of 10,000 partitions show a weaker association among subsets in the unrestricted comparison, whereas 4993 of 10,000 random partitions yield lower values in the comparison that is limited to spatially contiguous subsets. As in the test for the **G** matrix, the hypothesis of modularity is rejected for the **P** matrix.

Discussion

Our analyses have found pervasive integration for cranial shape in humans. Genetic variation is mostly concentrated in relatively few PCs featuring shape changes throughout the skull. Hypothetical selection consistently produces global responses to localized selection, with marked deflections of the evolutionary response from the direction of the selection gradient that manifest the effects of relative constraints. Finally, statistical testing suggests that the face, cranial base, and neurocranium do not behave as independent modules for either genetic or phenotypic shape variation that underscores the strong integration throughout the skull. Here, we evaluate these findings in the light of the results from other studies and discuss the implications for human evolution.

GENETIC INTEGRATION AND CONSTRAINT

The genetic and phenotypic variation of cranial shape is clearly structured, as morphological integration causes a concentration of the variation in relatively few dimensions (Fig. 3). As a result of this concentration, the potential for evolutionary change in response to selection will strongly depend on the direction of selection and, likewise, evolution by random drift will tend to be mainly in directions with large amounts of genetic variation (Lande 1979).

Allometry is widely known to act as an integrating factor in morphological structures (e.g., Klingenberg 2008, 2009). Because the allometric effects of size were removed by including centroid size as a covariate in the quantitative genetic model used to estimate the **G** matrix, allometry can be excluded as a factor responsible for the observed genetic integration.

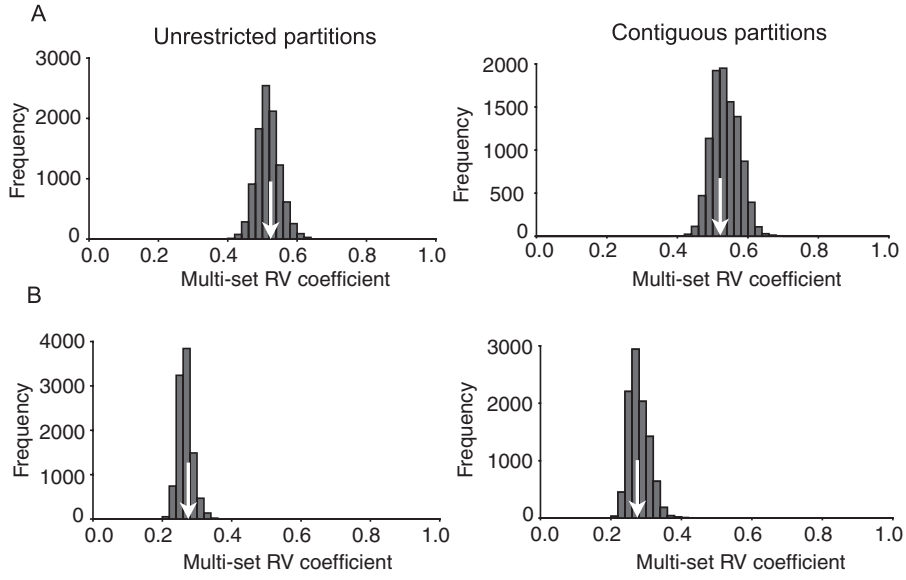

Figure 9. **Evaluation of the hypothesis that the face, cranial base, and cranial vault are separate modules. (A) Modularity in the G matrix. (B) Modularity in the P matrix. In each diagram, the white arrow indicates the multiset *RV* coefficient for the partition of landmarks according to the hypothesis (Fig. 2) and the histogram represents the distribution of multiset *RV* coefficients for 10,000 alternative partitions. For both matrices, comparisons used random partitions of the landmarks into subsets of 14, 7, and 8 landmarks without further restrictions (left diagrams) or with the additional condition that the partitions had to be spatially contiguous (right diagrams, see Fig. 2).**

Relative constraints: lines, planes, and subspaces of least resistance

Relative constraints have been discussed as the genetic line of least resistance (Schluter 1996) that is the PC1 of the **G** matrix. In our data, the shape change associated with the PC1 of the **G** matrix unites the four derived features of the modern human skull: shift of the foramen, retraction of the face, cranial flexion, and expansion of the neurocranium (Fig. 3C). This shape change, at least at the qualitative level of these four features, corresponds to the general trend in the human evolutionary lineage. Therefore, it is conceivable that human evolution to some extent followed the line of least resistance (Schluter 1996).

Such discussions of the lines of least resistance usually consider only the first PC of the **G** matrix or of the **P** matrix (Schluter 1996; Marroig and Cheverud 2005; Renaud et al. 2006; Hunt 2007). This exclusive focus on the first PC is not necessarily justified, as can be seen from our data on human cranial variation. Because the eigenvalue of the second PC of the **G** matrix is nearly as large as that of the first PC (Fig. 3A), the second PC also can have a substantial influence on evolutionary change. It is therefore possible to think of the two PCs together as defining a plane of least resistance. The response to selection will be deflected toward the direction of this plane. Depending on whether the direction of selection is closer to the first or second PC, one or the other will have a stronger effect in deflecting the response to selection. The shape change corresponding to the second PC (Fig. 3D), like the first PC, is also a combination of the key characters of modern humans. Because both PCs that define the plane of least resistance are related to these characters, the plane as a whole is also an expression of genetic integration throughout the skull. Of course, this line of thought can be continued by including the third and subsequent PCs, if they are deemed to account for sufficiently similar amounts of variation to the preceding PCs, resulting in a space of least resistance.

To evaluate the relative roles of all PCs of the **G** matrix, it is useful to consider the multivariate breeders' equation in combination with the spectral decomposition of the **G** matrix (e.g., Jolliffe 2002). This is the decomposition $\mathbf{G} = \mathbf{E}\mathbf{\Lambda}\mathbf{E}^{\mathrm{T}}$, where **E** is a square matrix whose columns are the eigenvectors of **G** (PC coefficients), $\mathbf{\Lambda}$ is the diagonal matrix of the eigenvalues of the **G** matrix, and the superscript "T" denotes transposition. Accordingly, the multivariate breeders' equation can be rewritten as

$$\Delta\mu = \mathbf{G}\boldsymbol{\beta} = \mathbf{E}\Lambda\mathbf{E}^{\mathrm{T}}\boldsymbol{\beta} = \sum_{i=1}^{p} \mathbf{e}_i \lambda_i \mathbf{e}_i^{\mathrm{T}}\boldsymbol{\beta} = \|\boldsymbol{\beta}\| \sum_{i=1}^{p} \mathbf{e}_i \lambda_i \cos\alpha_i,$$

where $\|\boldsymbol{\beta}\| = (\boldsymbol{\beta}^{\mathrm{T}}\boldsymbol{\beta})^{0.5}$ is the length of the selection gradient vector $\boldsymbol{\beta}$, $\mathbf{e}_i$ is the ith eigenvector of **G**, λ_i is the ith eigenvalue of **G**, α_i is the angle between $\mathbf{e}_i$ and $\boldsymbol{\beta}$, and p is the number of variables in the **G** matrix. The last expression writes the response to selection as a weighted sum, in which the effect of each eigenvector of **G** is weighted by the product of the corresponding eigenvalue and the cosine of the angle between that eigenvector and the selection gradient. This means that an eigenvector of **G** will only make a large contribution if the associated eigenvalue is relatively large

and if the angle between it and the selection gradient is relatively small (clearly less than a right angle, for which the cosine is zero). Overall, the influence of a "subspace of least resistance" is determined jointly by the angles between $\boldsymbol{\beta}$ and the eigenvectors that span the subspace and by the corresponding eigenvalues.

The angle of deflection of the evolutionary response from the direction of the selection gradient can be computed similarly. The cosine of the angle of deflection, δ, can be obtained as

$$\cos\delta = \frac{\boldsymbol{\beta}^{\mathrm{T}}}{\|\boldsymbol{\beta}\|}\frac{\Delta\boldsymbol{\mu}}{\|\Delta\boldsymbol{\mu}\|} = \frac{\sum_{i=1}^{p}(\cos\alpha_i)^2\lambda_i}{\sqrt{\sum_{i=1}^{p}(\cos\alpha_i)^2\lambda_i^2}}$$

This means that the angle of deflection is determined jointly by the angle between the selection gradient and each eigenvector of the **G** matrix and by the relative magnitude of the corresponding eigenvalue. There is no deflection (i.e., $\cos\delta = 1$) if $\boldsymbol{\beta}$ is in the direction of one of the eigenvectors of **G** (this also follows from the algebraic definition of eigenvectors). The maximum angle of deflection can approach, but not quite reach, 90° if $\boldsymbol{\beta}$ is nearly perpendicular to an eigenvector of **G** that accounts for most or all genetic variation (i.e., this requires extreme concentration of genetic variation in one or very few dimensions and it will result in a small magnitude of the response to selection). Because the angle of deflection is a function of the squared cosines of the angles α_i, the ability of each PC to deflect the selection response drops rapidly as the angle between $\boldsymbol{\beta}$ and that PC approaches a right angle (with cosine zero).

Extending the concept of lines of least resistance to subspaces is particularly relevant in the context of high-dimensional spaces, such as the shape spaces in geometric morphometrics. If the direction of selection is random relative to the genetic covariance structure, it is likely to be more or less perpendicular to the first PC of **G**, the line of least resistance, which therefore may not make a large contribution to the selection response. If there is a subspace of least resistance, however, where several PCs account for relatively large proportions of genetic variation of shape, chances are considerably greater that some combination of these PCs make a substantial contribution to the selection response. The observation that the PC2 of the **G** matrix in our dataset accounts for nearly as much variation as the PC1 (Fig. 3B) is an example of this.

RESPONSE TO SIMULATED SELECTION

All the simulations of selection produced results in which the direction of the evolutionary response was strongly deflected from the original direction of selection. This was apparent from the differences in shape features between selection gradients and the corresponding responses (Figs. 4–8) and directly from the angles between the selection gradients and the total responses to selection that are greater than 45° for all but one of our simulations. Accordingly, relative constraints appear to be important as a factor that can potentially affect evolutionary outcomes.

Localized selection consistently yielded a global response that involved the whole set of characters (Figs. 4–8). This global response reflects the strong genetic integration across the entire skull. This result is in agreement with previous studies using hypothetical selection in which selection for localized shape features produced responses throughout the entire structures under study (Klingenberg and Leamy 2001; Martínez-Abadías et al. 2009b; Klingenberg et al. 2010). It is also consistent with studies that found phenotypic integration throughout the human skull (Lieberman et al. 2000a; Bastir et al. 2005) and with analyses showing that localized artificial deformation affected the shape of the entire skull (Kohn et al. 1993; Martínez-Abadías et al. 2009b).

The selection gradients were constructed to reflect the principal derived features in the human skull (Aiello and Dean 1990; Lieberman et al. 2004, 2008; Bastir et al. 2010; Lieberman 2011). It is intriguing that selection for each of these features on its own tends to produce a response that contains the complete suite of features. The genetic integration throughout the skull produces a pattern of relative constraints where selection of any individual feature has the potential to facilitate the evolution of the others as well. Because qualitatively similar shape changes can result from different selection gradients, it is difficult to make inferences from evolutionary changes to the selection regime. This result is a reminder that interpretations about the selection pressures involved in human evolution must be made with caution (Lieberman 2008, 2011).

MODULARITY AND INTEGRATION

The analyses of modularity in the **G** the **P** matrices show that neither of them conforms to the hypothesis that the face, cranial vault, and cranial base are completely independent modules; instead, these structures are strongly integrated. For both covariance matrices, the covariation among subsets of landmarks according to this hypothesis is not weaker than covariation for other partitions, as would have been expected under the hypothesis (Fig. 9). This result holds regardless of whether the comparisons are limited to spatially contiguous subsets of landmarks or whether they were conducted without such a limitation. These results are inconsistent with the hypothesis of modularity.

There has been extensive discussion about the degree of interdependence between the face, cranial vault, and cranial base and whether these structures vary more or less independently from each other and can thus be considered as separate modules, or whether the entire skull behaves as a composite and strongly integrated structure and thus changes in one region will produce correlated phenotypic changes in other regions. Numerous studies in humans and other mammals have emphasized the modular nature of the skull and its possible role for evolution (e.g., Goswami

2006a, b; Bastir 2008; Cardini and Elton 2008; González-José et al. 2008; Mitteroecker and Bookstein 2008; Porto et al. 2009; Drake and Klingenberg 2010; Goswami and Polly 2010; Shirai and Marroig 2010; Jojić et al. 2011; Lieberman 2011). As the results obtained here do not support the hypothesis of complete modularity, they are similar to those from studies of modularity in mouse and newt skulls in which several hypotheses of modularity also were not supported by the data (Hallgrímsson et al. 2009; Ivanović and Kalezić 2010). Similar results of modularity tests were obtained in skull and circulatory structures in the head of mice (Jamniczky and Hallgrímsson 2011) and between brain regions in humans (Bruner et al. 2010). Moreover, even where modular variation has been found in skulls or other structures, between-module covariation often is not much weaker than within-module covariation that means that there is a degree of integration between modules (Klingenberg et al. 2003; Klingenberg 2009; Drake and Klingenberg 2010; Jojić et al. 2011).

That the first few PCs of the **G** and **P** matrices account for a substantial proportion of the total variance underscores that integration in the skull is fairly strong (Fig. 3A, B). This impression is reinforced by the observation that the shape changes associated with the first two PCs of the **G** matrix are not concentrated in particular regions, but affect the skull as a whole (Fig. 3C, D), indicating that there is genetic integration throughout the skull. Earlier studies have also provided clear evidence for integration in the human skull (e.g., Lieberman et al. 2000a; Bookstein et al. 2003; Mitteroecker and Bookstein 2008; Martínez-Abadías et al. 2009b; Bastir et al. 2010). The evolutionary consequences of this integration are clearly illustrated by the simulations of hypothetical selection.

A possible explanation why the covariance structure of shape is inconsistent with the hypothesis of modularity is that successive developmental processes produce different patterns of covariation that mutually obscure one another. Even though many processes that contribute to cranial variation may each act in a localized manner, there may not be a clear modular structure because the processes have effects in different but overlapping anatomical regions. Hallgrímsson et al. (2009) compared this process to a palimpsest in which older text on reused parchment has not been erased completely and appears under the new writing. The complex nature of the skull and its development provides many opportunities for such dynamic repatterning during ontogeny (e.g., Bastir 2008; Lieberman 2011).

A wide range of factors can contribute to genetic and environmental integration in the skull, including those that simultaneously affect processes in different parts of the developing head and epigenetic interactions that spread variation from a localized source through the whole head (Klingenberg 2005; Hallgrímsson et al. 2007; Klingenberg 2008; Hallgrímsson et al. 2009). Patterns of genetic and phenotypic integration may differ to the extent that developmental processes respond differentially to variation from different sources. For instance, mechanisms that act late in ontogeny may be more important for environmental integration because organisms may be more exposed to environmental variation late rather than early in development. Diet can be such a late-acting factor that influences growth of the skull by mechanical loading from mastication. Evidence that this process affects human skull shape comes from analyses of populations with different diets (Paschetta et al. 2010) and it also has been shown in experimental studies in mice (Renaud et al. 2010; Vecchione et al. 2010). Overall, genetic and environmental integration are expected to result from a combination of processes that act at different times and produce different patterns that are difficult to tease apart but may have important evolutionary implications (Hallgrímsson et al. 2009; Klingenberg 2010; Lieberman 2011).

Conclusions

Our analyses indicate that developmental integration in the skull, as it is manifest in the structure of the genetic and phenotypic covariance matrices, has a major effect on the outcome of selection and thus suggest that the adaptive context for the evolution of the human skull may need to be reinterpreted. Because relative constraints can produce substantial deflections of the evolutionary response from the direction of selection, inferring the selective pressures from observed changes in the fossil record is fraught with difficulty. It is conceivable that the derived characters of modern humans may not have arisen independently by adaptive evolution in response to separate selection pressures, but that the origin of one trait may have facilitated the evolution of the entire suite of characters. In this perspective, the developmental and genetic system plays an important role in human evolution and must be taken into account when considering selective factors that were involved (Lieberman 2008, 2011).

ACKNOWLEDGMENTS

We thank the authorities of Parish of Hallstatt, Institut für Anatomie (Innsbruck), Naturhistorisches Museum Wien, Musealverein Hallstatt, and Österreichisches Museum für Volkskunde (Wien) for permission to access their collections; and J. Cheverud, D. Lieberman, B. Wood, and three anonymous reviewers for helpful comments on earlier versions of the manuscript. This work was supported by the Wenner Gren Foundation for Anthropological Research, the Universitat de Barcelona and by the Spanish Ministerio de Educación y Ciencia MEC-FEDER (CGL2004–00903/BTE).

LITERATURE CITED

Ackermann, R. R., and J. M. Cheverud. 2004. Detecting genetic drift versus selection in human evolution. Proc. Natl. Acad. Sci. USA 101:17946–17951.

Adams, D. C. 2011. Quantitative genetics and evolution of head shape in *Plethodon* salamanders. Evol. Biol. 38:278–286.

Aiello, L., and C. Dean. 1990. An introduction to human evolutionary anatomy. Academic Press, London; San Diego, CA.

Arnold, S. J. 1992. Constraints on phenotypic evolution. Am. Nat. 140:S85–S107.

Arthur, W. 2001. Developmental drive: an important determinant of the direction of phenotypic evolution. Evol. Dev. 3:271–278.

Bastir, M. 2008. A systems-model for the morphological analysis of integration and modularity in human craniofacial evolution. J. Anthropol. Sci. 86:37–58.

Bastir, M., A. Rosas, and H. D. Sheets. 2005. The morphological integration of the hominoid skull: a partial least squares and PC analysis with implications for European Middle Pleistocene mandibular variation. Pp. 265–284 *in* D. Slice, ed. Modern Morphometrics in Physical Anthropology. Kluwer Academic/Plenum Publishers, New York.

Bastir, M., A. Rosas, C. B. Stringer, J. M. Cuétara, R. Kruszynski, G. W. Weber, C. F. Ross, and M. J. Ravosa. 2010. Effects of brain and facial size on basicranial form in human and primate evolution. J. Hum. Evol. 58:424–431.

Betti, L., F. Balloux, T. Hanihara, and A. Manica. 2010. The relative role of drift and selection shaping the human skull. Am. J. Phys. Anthropol. 141:76–82.

Bookstein, F. L., P. Gunz, P. Mitteroecker, H. Prossinger, K. Schaefer, and H. Seidler. 2003. Cranial integration in *Homo*: singular warps analysis of the midsagittal plane in ontogeny and evolution. J. Hum. Evol. 44:167–187.

Bruner, E., M. Martin-Loeches, and R. Colom. 2010. Human midsagittal brain shape variation: patterns, allometry and integration. J. Anat. 216:589–599.

Cardini, A., and S. Elton. 2008. Does the skull carry a phylogenetic signal? Evolution and modularity in the guenons. Biol. J. Linn. Soc. 93: 813–834.

Carson, E. A. 2006. Maximum likelihood estimation of human craniometric heritabilities. Am. J. Phys. Anthropol. 131:169–180.

Chenoweth, S. F., H. D. Rundle, and M. W. Blows. 2010. The contribution of selection and genetic constraints to phenotypic divergence. Am. Nat. 175:186–196.

Cheverud, J. M. 1984. Quantitative genetics and developmental constraints on evolution by selection. J. Theor. Biol. 110:155–171.

Drake, A. G., and C. P. Klingenberg. 2010. Large-scale diversification of skull shape in domestic dogs: disparity and modularity. Am. Nat. 175:289–301.

Dryden, I. L., and K. V. Mardia. 1998. Statistical shape analysis. Wiley, Chichester.

Escoufier, Y. 1973. Le traitement des variables vectorielles. Biometrics 29:751–760.

Evans, P. D., S. L. Gilbert, N. Mekel-Bobrov, E. J. Vallender, J. R. Anderson, L. M. Vaez-Azizi, S. A. Tishkoff, R. R. Hudson, and B. T. Lahn. 2005. *Microcephalin*, a gene regulating brain size, continues to evolve adaptively in humans. Science 309:1717–1720.

Futuyma, D. J. 2010. Evolutionary constraint and ecological consequences. Evolution 64:1865–1884.

González-José, R., I. Escapa, W. A. Neves, R. Cúneo, and H. M. Pucciarelli. 2008. Cladistic analysis of continuous modularized traits provides phylogenetic signals in *Homo* evolution. Nature 453: 775–778.

Goswami, A. 2006a. Cranial modularity shifts during mammalian evolution. Am. Nat. 168:270–280.

———. 2006b. Morphological integration in the carnivoran skull. Evolution 60:169–183.

Goswami, A., and P. D. Polly. 2010. The influence of modularity on cranial morphological disparity in Carnivora and Primates (Mammalia). PLoS One 5:e9517.

Gould, S. J. 2002. The structure of evolutionary theory. Harvard Univ. Press, Cambridge, MA.

Groeneveld, E., M. Kovač, and N. Mielenz. 2008. VCE user's guide and reference manual, version 6.0. Institute of Farm Animal Genetics, Neustadt, Germany.

Hallgrímsson, B., H. A. Jamniczky, N. M. Young, C. Rolian, T. E. Parsons, J. C. Boughner, and R. S. Marcucio. 2009. Deciphering the palimpsest: studying the relationship between morphological integration and phenotypic covariation. Evol. Biol. 36:355–376.

Hallgrímsson, B., D. E. Lieberman, W. Liu, A. F. Ford-Hutchinson, and F. R. Jirik. 2007. Epigenetic interactions and the structure of phenotypic variation in the cranium. Evol. Dev. 9:76–91.

Hernandez, R. D., J. L. Kelley, E. Elyashiv, S. C. Melton, A. Auton, G. McVean, 1000 Genomes Project, G. Sella, and M. Przeworski. 2011. Classic selective sweeps were rare in recent human evolution. Science 331:920–924.

Hoekstra, H. E., J. M. Hoekstra, D. Berrigan, S. N. Vignieri, A. Hoang, C. E. Hill, P. Beerli, and J. G. Kingsolver. 2001. Strength and tempo of directional selection in the wild. Proc. Natl. Acad. Sci. USA 98:9157–9160.

Hunt, G. 2007. Evolutionary divergence in directions of high phenotypic variance in the ostracode genus *Poseidonamicus*. Evolution 61:1560–1576.

Ivanović, A., and M. L. Kalezić. 2010. Testing the hypothesis of morphological integration on a skull of a vertebrate with a biphasic life cycle: a case study of the alpine newt. J. Exp. Zool. B Mol. Dev. Evol. 314: 527–538.

Jaanusson, V. 1987. Balance of the human head in hominid evolution. Lethaia 20:165–176.

Jamniczky, H. A., and B. Hallgrímsson. 2011. Modularity in the skull and cranial vasculature of laboratory mice: implications for the evolution of complex phenotypes. Evol. Dev. 13;28–37.

Johannsdottir, B., F. Thorarinsson, A. Thordarson, and T. E. Magnusson. 2005. Heritability of craniofacial characteristics between parents and offspring estimated from lateral cephalograms. Am. J. Orthod. Dentofacial Orthop. 127:200–207.

Jojić, V., J. Blagojević, and M. Vujošević. 2011. B chromosomes and cranial variability in yellow-necked field mice (*Apodemus flavicollis*). J. Mammal. 92:396–406.

Jolliffe, I. T. 2002. Principal component analysis. Springer-Verlag, New York.

Kingsolver, J. G., H. E. Hoekstra, J. M. Hoekstra, D. Berrigan, S. N. Vignieri, C. E. Hill, A. Hoang, P. Gibert, and P. Beerli. 2001. The strength of phenotypic selection in natural populations. Am. Nat. 157: 245–261.

Kirkpatrick, M. 2009. Patterns of quantitative genetic variation in multiple dimensions. Genetica (Dordr.) 136:271–284.

Klingenberg, C. P. 2005. Developmental constraints, modules and evolvability. Pp. 219–247 *in* B. Hallgrímsson and B. K. Hall, eds. Variation: a central concept in biology. Elsevier, Burlington, MA.

———. 2008. Morphological integration and developmental modularity. Annu. Rev. Ecol. Evol. Syst. 39:115–132.

———. 2009. Morphometric integration and modularity in configurations of landmarks: tools for evaluating a-priori hypotheses. Evol. Dev. 11;405–421.

———. 2010. Evolution and development of shape: integrating quantitative approaches. Nat. Rev. Genet. 11:623–635.

———. 2011. MorphoJ: an integrated software package for geometric morphometrics. Mol. Ecol. Res. 11:353–357.

Klingenberg, C. P., V. Debat, and D. A. Roff. 2010. Quantitative genetics of shape in cricket wings: developmental integration in a functional structure. Evolution 64:2935–2951.

Klingenberg, C. P., and L. J. Leamy. 2001. Quantitative genetics of geometric shape in the mouse mandible. Evolution 55:2342–2352.

Klingenberg, C. P., and G. S. McIntyre. 1998. Geometric morphometrics of developmental instability: analyzing patterns of fluctuating asymmetry with Procrustes methods. Evolution 52:1363–1375.

Klingenberg, C. P., K. Mebus, and J.-C. Auffray. 2003. Developmental integration in a complex morphological structure: how distinct are the modules in the mouse mandible? Evol. Dev. 5:522–531.

Klingenberg, C. P., and L. R. Monteiro. 2005. Distances and directions in multidimensional shape spaces: implications for morphometric applications. Syst. Biol. 54:678–688.

Kohn, L. A., S. R. Leigh, S. C. Jacobs, and J. M. Cheverud. 1993. Effects of annular cranial vault modification on the cranial base and face. Am. J. Phys. Anthropol. 90:147–168.

Kruuk, L. E. B. 2004. Estimating genetic parameters in natural populations using the 'animal model'. Philos. Trans. R. Soc. Lond. B 359:873–890.

Kruuk, L. E. B., J. Slate, and A. J. Wilson. 2008. New answers for old questions: the evolutionary quantitative genetics of wild animal populations. Annu. Rev. Ecol. Evol. Syst. 39:525–548.

Lande, R. 1979. Quantitative genetic analysis of multivariate evolution, applied to brain: body size allometry. Evolution 33:402–416.

Lande, R., and S. J. Arnold. 1983. The measurement of selection on correlated characters. Evolution 37:1210–1226.

Leinonen, T., J. M. Cano, and J. Merilä. 2011. Genetics of body shape and armour variation in threespine sticklebacks. J. Evol. Biol. 24: 206–218.

Lieberman, D. E. 2008. Speculations about the selective basis for modern human craniofacial form. Evol. Anthropol. 17:55–68.

———. 2011. The evolution of the human head. Harvard Univ. Press, Cambridge, MA.

Lieberman, D. E., B. Hallgrímsson, W. Liu, T. E. Parsons, and H. A. Jamniczky. 2008. Spatial packing, cranial base angulation, and craniofacial shape variation in the mammalian skull: testing a new model using mice. J. Anat. 212:720–735.

Lieberman, D. E., G. E. Krovitz, and B. M. McBratney-Owen. 2004. Testing hypotheses about tinkering in the fossil record: the case of the human skull. J. Exp. Zool. B 302:284–301.

Lieberman, D. E., O. M. Pearson, and K. M. Mowbray. 2000a. Basicranial influence on overall cranial shape. J. Hum. Evol. 38:291–315.

Lieberman, D. E., C. F. Ross, and M. J. Ravosa. 2000b. The primate cranial base: ontogeny, function, and integration. Yearb. Phys. Anthropol. 43:117–169.

Lynch, M., and B. Walsh. 1998. Genetics and analysis of quantitative traits. Sinauer, Sunderland, MA.

Marroig, G., and J. M. Cheverud. 2005. Size as a line of least evolutionary resistance: diet and adaptive morphological radiation in New World monkeys. Evolution 59:1128–1142.

Martínez-Abadías, N., M. Esparza, T. Sjøvold, R. González-José, M. Santos, and M. Hernández. 2009a. Heritability of human cranial dimensions: comparing the evolvability of different cranial regions. J. Anat. 214:19–35.

Martínez-Abadías, N., C. Paschetta, S. de Azevedo, M. Esparza, and R. González-José. 2009b. Developmental and genetic constraints on neurocranial globularity: insights from analyses of deformed skulls and quantitative genetics. Evol. Biol. 36:37–56.

Maynard Smith, J., R. Burian, S. Kauffman, P. Alberch, J. Campbell, B. Goodwin, R. Lande, D. Raup, and L. Wolpert. 1985. Developmental constraints and evolution. Q. Rev. Biol. 60:265–287.

McLean, C. Y., P. L. Reno, A. A. Pollen, A. I. Bassan, T. D. Capellini, C. Guenther, V. B. Indjeian, X. Lim, D. B. Menke, B. T. Schaar, et al. 2011. Human-specific loss of regulatory DNA and the evolution of human-specific traits. Nature 471:216–219.

Mekel-Bobrov, N., S. L. Gilbert, P. D. Evans, E. J. Vallender, J. R. Anderson, R. R. Hudson, S. A. Tishkoff, and B. T. Lahn. 2005. Ongoing adaptive evolution of *ASPM*, a brain size determinant in *Homo sapiens*. Science 309:1720–1722.

Meyer, K. 2007. WOMBAT—A tool for mixed model analyses in quantitative genetics by restricted maximum likelihood (REML). J. Zhejiang Univ. Sci. B. 8:815–821.

Mitteroecker, P., and F. L. Bookstein. 2008. The evolutionary role of modularity and integration in the hominoid cranium. Evolution 62:943–958.

Myers, E. M., F. J. Janzen, D. C. Adams, and J. K. Tucker. 2006. Quantitative genetics of plastron shape in slider turtles (*Trachemys scripta*). Evolution 60:563–572.

Paschetta, C., S. De Azevedo, L. Castillo, N. Martínez-Abadías, M. Hernández, D. E. Lieberman, and R. González-José. 2010. The influence of masticatory loading on craniofacial morphology: a test case across technological transitions in the Ohio valley. Am. J. Phys. Anthropol. 141:297–314.

Perez, S. I., and L. R. Monteiro. 2009. Nonrandom factors in modern human morphological diversification: a study of craniofacial variation in southern South American populations. Evolution 63:978–993.

Pollard, K. S., S. R. Salama, N. Lambert, M.-A. Lambot, S. Coppens, J. S. Pedersen, S. Katzman, B. King, C. Onodera, A. Siepel, et al. 2006. An RNA gene expressed during cortical development evolved rapidly in humans. Nature 443:167–172.

Porto, A., F. B. De Oliveira, L. T. Shirai, V. De Conto, and G. Marroig. 2009. The evolution of modularity in the mammalian skull I: morphological integration patterns and magnitudes. Evol. Biol. 36:118–135.

Renaud, S., J.-C. Auffray, and S. de la Porte. 2010. Epigenetic effects on the mouse mandible: common features and discrepancies in remodeling due to muscular dystrophy and response to food consistency. BMC Evol. Biol. 10:28.

Renaud, S., J.-C. Auffray, and J. Michaux. 2006. Conserved phenotypic variation patterns, evolution along lines of least resistance, and departure due to selection in fossil rodents. Evolution 60:1701–1717.

Roff, D. A. 1997. Evolutionary quantitative genetics. Chapman & Hall, New York.

Roseman, C. C. 2004. Detecting interregionally diversifying natural selection on modern human cranial form by using matched molecular and morphometric data. Proc. Natl. Acad. Sci. USA 101: 12824–12829.

Schluter, D. 1996. Adaptive radiation along genetic lines of least resistance. Evolution 50:1766–1774.

Sherwood, R. J., D. L. Duren, E. W. Demerath, S. A. Czerwinski, R. M. Siervogel, and B. Towne. 2008. Quantitative genetics of modern human cranial variation. J. Hum. Evol. 54:909–914.

Shirai, L. T., and G. Marroig. 2010. Skull modularity in Neotropical marsupials and monkeys: size variation and evolutionary constraint and flexibility. J. Exp. Zool. B 314:663–683.

Sjøvold, T. 1984. A report on the heritability of some cranial measurements and non-metric traits. Pp. 223–246 *in* G. N. Van Vark and W. W. Howells, eds. Multivariate statistical methods in Physical Anthropology. Reidel Publishing Company, Dordrecht.

Stedman, H. H., B. W. Kozyak, A. Nelson, D. M. Thesier, L. T. Su, D. W. Low, C. R. Bridges, J. B. Shrager, N. Minugh-Purvis, and M. A. Mitchell.

2004. Myosin gene mutation correlates with anatomical changes in the human lineage. Nature 428:415–418.

Tennessen, J. A., and J. M. Akey. 2011. Parallel adaptive divergence among geographically diverse human populations. PLoS Genet. 7:e1002127.

Vecchione, L., J. Miller, C. Byron, G. M. Cooper, T. Barbano, J. Cray, J. E. Losee, M. W. Hamrick, J. J. Sciote, and M. P. Mooney. 2010. Age-related changes in craniofacial morphology in GDF-8 (myostatin)-deficient mice. Anat. Rec. 293:32–41.

von Cramon-Taubadel, N. 2009. Congruence of individual cranial bone morphology and neutral molecular affinity patterns in modern humans. Am. J. Phys. Anthropol. 140:205–215.

Walsh, B., and M. W. Blows. 2009. Abundant genetic variation + strong selection = multivariate genetic constraints: a geometric view of adaptation. Annu. Rev. Ecol. Evol. Syst. 40:41–59.

Weaver, T. D., C. C. Roseman, and C. B. Stringer. 2007. Were neandertal and modern human cranial differences produced by natural selection or genetic drift? J. Hum. Evol. 53:135–145.

Wilson, A. J., D. Réale, M. N. Clements, M. M. Morrissey, E. Postma, C. A. Walling, L. E. B. Kruuk, and D. H. Nussey. 2010. An ecologist's guide to the animal model. J. Anim. Ecol. 79:13–26.

Associate Editor: N. Barton

Supporting Information

The following supporting information is available for this article:

Table S1. List of digitized landmarks and brief anatomical definitions.
Table S2. Mean shape configuration: 3D landmark coordinates after generalized Procrustes superimposition.
Table S3. Selection gradient for bipedalism.
Table S4. Selection gradient for cranial base flexion.
Table S5. Selection gradient for facial retraction.
Table S6. Selection gradient for anterior enlargement of the cranial vault.
Table S7. Selection gradient for posterior enlargement of the cranial vault.

Supporting Information may be found in the online version of this article.